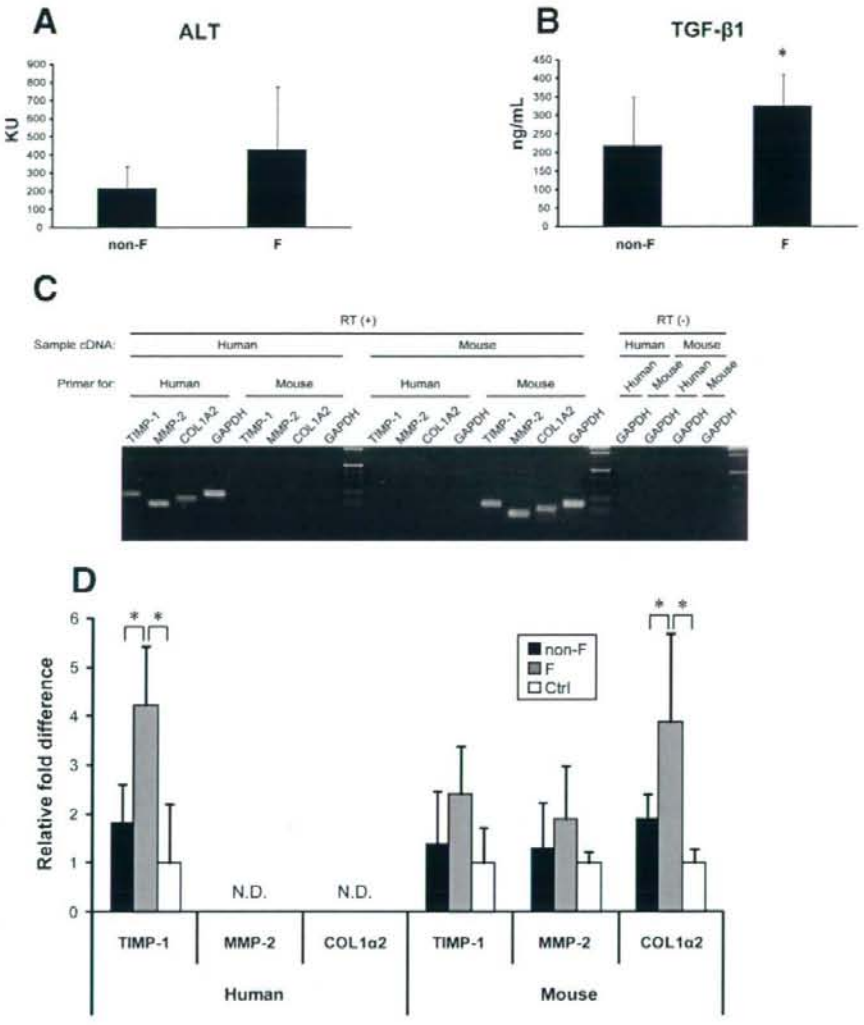

Figure 6. Differences in the expression levels of fibrosis-related genes among HBV genotypes. Quantification of (*A*) ALT and (*B*) TGF-β1 levels in mouse sera with enzyme-linked immunosorbent assay (see Supplementary Materials and Methods section. non-F, no fibrosis group (A2 and B1_wild); F, fibrosis group (C2 and B1_PCm). *$P < .01$: non-F vs F. (*C*) The specificity of each PCR using species-specific primer sets. The species-specific primer sets were established to determine whether mRNA of fibrosis-related genes were of human or mouse origin. Liver tissue of a HCC patient or a mouse without transplantation of human hepatocytes was used to check the primer sets for real-time detection PCR. The PCR products were run on 2% agarose gels to confirm the molecular sizes as well as species-specific amplifications. (*D*) Quantification of mRNA expression on fibrosis-related genes in each group by real-time reverse-transcription PCR. non-F group, n = 15; F group, n = 22; control, n = 8; ND, not detected; *$P < .001$.

Finally, the discrepancy between in vitro[21] and in vivo (present study) observations on HBV/B1_wild might have been caused by differences in the cells used for transfection (Huh7 cells) and infection (human hepatocytes from Caucasoid donors), respectively. Nonrecombinant type HBV/B strains (B1 and B6) have been detected in limited areas including Japan[44] and Alaska,[45] which were settled mainly by Mongoloid people. The existence of a window period on HBV/B1 might indicate a possibility that a receptor or co-receptor used by HBV/B1 is not equal to one adopted by other genotypes as shown in the human herpes virus.[46] Further studies using human hepatocytes from Mongoloid people would be required.

In conclusion, using an in vivo experimental system, we show that different HBV genotypes and even particular mutations are associated with different virologic and histopathologic characteristics. Infection with HBV/C2 as well as PC mutant of the HBV/B1 in immunosuppressive conditions can induce a direct cytopathic effect in the humanized part of the murine liver. This mouse model appears to be useful in the evaluation and prediction of pathogenic effects of various genotypes of HBV and certain HBV mutations.

Supplementary Data

Note: To access the supplementary material accompanying this article, visit the online version of *Gastroenterology* at www.gastrojournal.org, and at doi: 10.1053/j.gastro.2008.10.048.

References

1. Mast EE, Alter MJ, Margolis HS. Strategies to prevent and control hepatitis B and C virus infections: a global perspective. Vaccine 1999;17:1730–1733.
2. Meuleman P, Libbrecht L, Wieland S, et al. Immune suppression uncovers endogenous cytopathic effects of the hepatitis B virus. J Virol 2006;80:2797–2807.
3. Sugiyama M, Tanaka Y, Sakamoto T, et al. Early dynamics of hepatitis B virus in chimeric mice carrying human hepatocytes monoinfected or coinfected with genotype G. Hepatology 2007; 45:929–937.
4. Orito E, Mizokami M. Hepatitis B virus genotypes and hepatocellular carcinoma in Japan. Intervirology 2003;46:408–412.
5. Pujol FH, Devesa M. Genotypic variability of hepatitis viruses associated with chronic infection and the development of hepatocellular carcinoma. J Clin Gastroenterol 2005;39:611–618.
6. Norder H, Courouce AM, Coursaget P, et al. Genetic diversity of hepatitis B virus strains derived worldwide: genotypes, subgenotypes, and HBsAg subtypes. Intervirology 2004;47:289–309.
7. Kramvis A, Kew MC. Relationship of genotypes of hepatitis B virus to mutations, disease progression and response to antiviral therapy. J Viral Hepat 2005;12:456–464.
8. Liu CJ, Kao JH, Chen DS. Therapeutic implications of hepatitis B virus genotypes. Liver Int 2005;25:1097–1107.
9. Miyakawa Y, Mizokami M. Classifying hepatitis B virus genotypes. Intervirology 2003;46:329–338.
10. Schaefer S. Hepatitis B virus: significance of genotypes. J Viral Hepat 2005;12:111–124.
11. Ozasa A, Tanaka Y, Orito E, et al. Influence of genotypes and precore mutations on fulminant or chronic outcome of acute hepatitis B virus infection. Hepatology 2006;44:326–334.
12. Tanaka Y, Hasegawa I, Kato T, et al. A case-control study for differences among hepatitis B virus infections of genotypes A (subtypes Aa and Ae) and D. Hepatology 2004;40:747–755.
13. Tanaka Y, Mukaide M, Orito E, et al. Specific mutations in enhancer II/core promoter of hepatitis B virus subgenotypes C1/C2 increase the risk of hepatocellular carcinoma. J Hepatol 2006; 45:646–653.
14. Kremsdorf D, Soussan P, Paterlini-Brechot P, et al. Hepatitis B virus-related hepatocellular carcinoma: paradigms for viral-related human carcinogenesis. Oncogene 2006;25:3823–3833.
15. Tong SP, Li JS, Vitvitski L, et al. Replication capacities of natural and artificial precore stop codon mutants of hepatitis B virus: relevance of pregenome encapsidation signal. Virology 1992; 191:237–245.
16. Heckel JL, Sandgren EP, Degen JL, et al. Neonatal bleeding in transgenic mice expressing urokinase-type plasminogen activator. Cell 1990;62:447–456.
17. Rhim JA, Sandgren EP, Degen JL, et al. Replacement of diseased mouse liver by hepatic cell transplantation. Science 1994;263: 1149–1152.
18. Tateno C, Yoshizane Y, Saito N, et al. Near completely humanized liver in mice shows human-type metabolic responses to drugs. Am J Pathol 2004;165:901–912.
19. Mercer DF, Schiller DE, Elliott JF, et al. Hepatitis C virus replication in mice with chimeric human livers. Nat Med 2001;7:927–933.
20. Tsuge M, Hiraga N, Takaishi H, et al. Infection of human hepatocyte chimeric mouse with genetically engineered hepatitis B virus. Hepatology 2005;42:1046–1054.
21. Sugiyama M, Tanaka Y, Kato T, et al. Influence of hepatitis B virus genotypes on the intra- and extracellular expression of viral DNA and antigens. Hepatology 2006;44:915–924.
22. Yuan TT, Sahu GK, Whitehead WE, et al. The mechanism of an immature secretion phenotype of a highly frequent naturally occurring missense mutation at codon 97 of human hepatitis B virus core antigen. J Virol 1999;73:5731–5740.
23. Chua PK, Wang RY, Lin MH, et al. Reduced secretion of virions and hepatitis B virus (HBV) surface antigen of a naturally occurring HBV variant correlates with the accumulation of the small S envelope protein in the endoplasmic reticulum and Golgi apparatus. J Virol 2005;79:13483–13496.
24. Harrison-Findik DD, Schafer D, Klein E, et al. Alcohol metabolism-mediated oxidative stress down-regulates hepcidin transcription and leads to increased duodenal iron transporter expression. J Biol Chem 2006;281:22974–22982.
25. Takahashi S, Hirose M, Tamano S, et al. Immunohistochemical detection of 8-hydroxy-2'-deoxyguanosine in paraffin-embedded sections of rat liver after carbon tetrachloride treatment. Toxicol Pathol 1998;26:247–252.
26. Purohit V, Brenner DA. Mechanisms of alcohol-induced hepatic fibrosis: a summary of the Ron Thurman Symposium. Hepatology 2006;43:872–878.
27. Ramirez F, Di Liberto M. Complex and diversified regulatory programs control the expression of vertebrate collagen genes. FASEB J 1990;4:1616–1623.
28. Orito E, Mizokami M, Sakugawa H, et al. A case-control study for clinical and molecular biological differences between hepatitis B viruses of genotypes B and C. Japan HBV Genotype Research Group. Hepatology 2001;33:218–223.
29. Sumi H, Yokosuka O, Seki N, et al. Influence of hepatitis B virus genotypes on the progression of chronic type B liver disease. Hepatology 2003;37:19–26.
30. Heijtink RA, Paulij W, van Roosmalen M, et al. Characteristics of the early phase of chronicity in acute hepatitis B infection. J Med Virol 1999;57:331–336.
31. Kobayashi M, Arase Y, Ikeda K, et al. Viral genotypes and response to interferon in patients with acute prolonged hepatitis B virus infection of adulthood in Japan. J Med Virol 2002;68:522–528.
32. Lindh M, Horal P, Norkrans G. Acute hepatitis B in Western Sweden—genotypes and transmission routes. Infection 2000; 28:161–163.
33. Chisari FV, Ferrari C. Hepatitis B virus immunopathogenesis. Annu Rev Immunol 1995;13:29–60.
34. Chen CH, Chen PJ, Chu JS, et al. Fibrosing cholestatic hepatitis in a hepatitis B surface antigen carrier after renal transplantation. Gastroenterology 1994;107:1514–1518.
35. Lok AS, Liang RH, Chiu EK, et al. Reactivation of hepatitis B virus replication in patients receiving cytotoxic therapy. Report of a prospective study. Gastroenterology 1991;100:182–188.
36. Dandri M, Burda MR, Torok E, et al. Repopulation of mouse liver with human hepatocytes and in vivo infection with hepatitis B virus. Hepatology 2001;33:981–988.
37. Meuleman P, Libbrecht L, De Vos R, et al. Morphological and biochemical characterization of a human liver in a uPA-SCID mouse chimera. Hepatology 2005;41:847–856.
38. Kobayashi M, Arase Y, Ikeda K, et al. Clinical characteristics of patients infected with hepatitis B virus genotypes A, B, and C. J Gastroenterol 2002;37:35–39.
39. Murokawa H, Yoshikawa A, Ohnuma H, et al. Epidemiology of blood donors in Japan, positive for hepatitis B virus and hepatitis C virus by nucleic acid amplification testing. Vox Sang 2005;88: 10–16.
40. Liang TJ, Hasegawa K, Rimon N, et al. A hepatitis B virus mutant associated with an epidemic of fulminant hepatitis. N Engl J Med 1991;324:1705–1709.
41. Omata M, Ehata T, Yokosuka O, et al. Mutations in the precore region of hepatitis B virus DNA in patients with fulminant and severe hepatitis. N Engl J Med 1991;324:1699–1704.

42. Milich D, Liang TJ. Exploring the biological basis of hepatitis B e antigen in hepatitis B virus infection. Hepatology 2003;38:1075–1086.
43. Bocharov G, Ludewig B, Bertoletti A, et al. Underwhelming the immune response: effect of slow virus growth on CD8+-T-lymphocyte responses. J Virol 2004;78:2247–2254.
44. Sugauchi F, Orito E, Ichida T, et al. Epidemiologic and virologic characteristics of hepatitis B virus genotype B having the recombination with genotype C. Gastroenterology 2003;124:925–932.
45. Sakamoto T, Tanaka Y, Simonetti J, et al. Classification of hepatitis B virus genotype B into two major types based on characterization of a novel subgenotype in the Arctic indigenous populations. J Infect Dis 2007;196:1487–1492.
46. Mori Y, Seya T, Huang HL, et al. Human herpesvirus 6 variant A but not variant B induces fusion from without in a variety of human cells through a human herpesvirus 6 entry receptor, CD46. J Virol 2002;76:6750–6761.

Received April 20, 2008. Accepted October 23, 2008.

Address requests for reprints to: Masashi Mizokami, MD, PhD, Department of Clinical Molecular Informative Medicine, Nagoya City University Graduate School of Medical Sciences, Kawasumi, Mizuho, Nagoya 467-8601, Japan . e-mail: mizokami@med.nagoya-cu.ac.jp; fax: (81) 52-842-0021.

The authors disclose the following: Supported by a grant-in-aid from the Ministry of Education, Culture, Sports, Science, and Technology, and a grant-in-aid from the Ministry of Health, Labour, and Welfare of Japan, the Toyoaki Foundation.

The authors thank Drs C. Tateno, H. Yokomichi, K. Kuramoto, and T. Nakamura of PhoenixBio Co, Ltd for providing chimeric mice with a high replacement for hepatocytes; Dr T. Wakita of the National Institute of Infectious Diseases, Tokyo, Japan for quantifying the alanine aminotransferase level; Dr Ikehara of the National Institute of Advanced Industrial Science and Technology for the differential diagnosis of neutrophil/monocyte in liver tissue; Dr S. Nishina of Yamaguchi University Graduate School of Medicine for assistance with histological reactive oxygen species evaluation; Ms K. Tatematsu of Nagoya City University Graduate School of Medical Sciences for performing sequencing; and Mr S. Sato and Ms Y. Tanizaki of Nagoya City University Hospital for slicing liver tissues of chimeric mice.

The nucleotide sequences of HBV-DNA isolates used in this study have been deposited in the international DNA database under the following accession numbers: AB246337, AB246338, AB246341, AB246342, AB246344, AB246345, and AB362931–362933.

Supplementary Data

Materials and Methods

Plasmid Constructs of HBV DNA and Sequencing

The 1.24-fold HBV genomic constructs used in the present study were prepared as described previously.[1] The constructs were designed to transcribe oversized pregenome and precore mRNA. Table 1 shows the list of 12 plasmids used in this study. Nine wild-type clones were used including 3 HBV/A (Ae/A2), 3 HBV/B (Bj/B1), and 3 HBV/C (Ce/C2). An additional 3 HBV/B plasmids identical to the earlier-mentioned HBV/B clone were constructed with precore stop-codon (PC) mutation (G1896A), which abolishes HBeAg expression. Briefly, for site-directed mutagenesis, the wild-type clone was digested by *Hind*III and *EcoO65*I and ligated with the fragment carrying the PC mutation (G1896A). Cloned HBV-DNA sequences were confirmed with Prism Big Dye (Applied Biosystems, Foster City, CA) in the ABI 3100 automated sequencer. Furthermore, the HBV DNA spanning the complete genome were amplified from murine sera and cloned into the pGEM-T Easy Vector (Applied Biosystems) with followed sequencing.

Cell Culture and Transfection

Huh7 cells were transfected with plasmids equivalent to 5 μg of HBV-DNA constructs with use of the Fugene 6 transfection reagent (Roche Diagnostics, Indianapolis, IN), and harvested after 3 days in culture. Transfection efficiency was monitored by cotransfecting 0.5 μg of reporter plasmids expressing secreted alkaline phosphatase in the culture media.

Determination of HBV Markers

HBsAg and HBeAg were determined by chemiluminescent enzyme immunoassay using commercial kits (Fujirebio Inc, Tokyo, Japan). HBcrAgs, which included both HBeAg and HBcAg, were measured in serum using the chemiluminescent enzyme immunoassay as described previously.[2,3] HBcAg was measured by enzyme-linked immunosorbent assay as previously reported.[2]

Detection and Quantification of Serum HBV DNA

HBV-DNA sequences spanning the S gene were amplified by real-time detection PCR by the method of Abe et al.[4] The detection threshold of the method is 100 copies/mL (equivalent to 20 IU/mL). However, because of the small volume of the serum available from each mouse for the HBV-DNA quantification, 10-fold template dilution was used, which resulted in a higher detection threshold of the method in this study: 1000 copies/mL (200 IU/mL). Quantification standards used in the assay were prepared based on World Health Organization standard serum containing HBV genotype A (kindly provided by Dr Hiroshi Yoshizawa of Hiroshima University). The amplification and detection were performed in the ABI Prism 7700 Sequence Detection System (Applied Biosystems) according to the protocol.

Detection of 8-OHdG in Liver Tissue

The slides obtained from frozen tissues for 8-OHdG determination were placed in Bouin's fixative overnight at room temperature, and washed in water for 20 minutes. Tissues were incubated with 0.3% H_2O_2 in methanol for 30 minutes and rinsed in phosphate-buffered saline (PBS) buffer. The slides were placed in 0.05 N NaOH in 40% ethanol for 12 minutes, rinsed in PBS, and incubated with 250 μg/mL ribonuclease for 1 hour. An avidin/biotin block (Vector Laboratories) was applied for 20 minutes, and super block and mouse-to-mouse blocking reagent (ScyTek Laboratories, Logan, UT) were used to eliminate background staining caused by endogenous mouse immunoglobulin (Ig)G. The primary 8-OHdG antibody (Japan Institute for the Control of Aging, Shizuoka, Japan) then was applied to the slides overnight at 4°C (20 μg/mL, 1:100). To detect positive cells binding primary antibody, these slides were treated with Vectastain Elite ABC kit (Vector Laboratories).

Quantification of TGF-β1 and ALT Levels in Sera

Serum TGF-β1 and ALT levels were determined by using commercially available enzyme-linked immunoassay kits (Bender MedSystems GmbH, Vienna, Austria; and Nissui Pharmaceutical Co, LTD, Tokyo, Japan) according to the manufacturer's instructions, respectively.

Quantification of Gene Expression Levels of Fibrosis Markers

Fresh liver tissues (n = 45) from killed mice were used for quantification of fibrosis markers. Total RNAs were isolated using the RNeasy Mini Kit, and DNA contamination of samples was eliminated using the RNase-free DNase Set (Qiagen, Hilden, Germany), according to the manufacturer's instructions. First-strand complementary DNA (cDNA) was synthesized in reaction mixtures with SuperScript II RNase H⁻ Reverse Transcriptase kit (Invitrogen), adding 0.5 μg oligo(dT)$_{12-18}$ primer at 70°C for 10 minutes. Reaction mixtures were incubated sequentially at 42°C for 60 minutes, at 95°C for 5 minutes, and at 60°C for 5 minutes. To check DNA contamination of samples, PCR was performed using isolated samples without reverse transcriptase. Primer sets to detect species-specific cDNA were designed using Primer Express software (Applied Biosystems) and are shown in Supplementary Table 1. Equal aliquots (1 μL) of cDNA were amplified by real-time detection PCR according to the manufacturer's Power SYBR Green PCR Master Mix instructions (Applied Biosystems) using the ABI Prism 7700 Sequence Detection System (Applied

Biosystems) in triplicate. The PCR conditions were as follows: (1) stage 1, 50°C for 2 minutes; (2) stage 2, 95°C for 10 minutes; and (3) stage 3, 95°C for 15 seconds followed by amplification at 60°C for 1 minute. Stage 3 was repeated for 40 cycles. Specificity of the amplification products was confirmed by examination of dissociation reaction plots, and a distinct single peak indicated a single DNA sequence amplified by the real-time detection PCR. The PCR products were run on 2% agarose gels to confirm the molecular sizes as well as species-specific amplifications (Figure 6C). Data were analyzed by the 2 [-Delta Delta C(t)] method using Sequence Detector version 1.7 software (Applied Biosystems),[5] and were normalized using human or mouse-specific glyceraldehyde-3-phosphate dehydrogenase. A standard curve was prepared by serial 10-fold dilutions of human or mouse cDNA. The curve was linear over 7 logs with a 0.998 correlation coefficient.

Immunofluorescence Immunofluorescence was performed as previously reported.[1] Briefly, fresh-frozen specimens were cut at 5–6 μm by cryostat, and fixed in acetone at room temperature for 10 minutes. Liver sections were blocked with Antibody Diluent (Dako, Glostrup, Denmark), incubated with rabbit anti-HBc antibody (Dako) at room temperature for 1 hour, and then incubated with goat anti-rabbit IgG antibody conjugated with Cy3 (Chemicon) or goat anti-human albumin antibody labeled with FITC (Bethyl Laboratories Inc, Montgomery, TX). Sections were observed in a fluorescent microscopy (Eclipse E800M; Nikon, Tokyo, Japan).

Statistical Analysis

Group means were compared by an independent Student *t* test or 1-way analysis of variance.

References

1. Sugiyama M, Tanaka Y, Kato T, et al. Influence of hepatitis B virus genotypes on the intra- and extracellular expression of viral DNA and antigens. Hepatology 2006;44:915–924.
2. Kimura T, Ohno N, Terada N, et al. Hepatitis B virus DNA-negative dane particles lack core protein but contain a 22-kDa precore protein without C-terminal arginine-rich domain. J Biol Chem 2005; 280:21713–21719.
3. Shinkai N, Tanaka Y, Orito E, et al. Measurement of hepatitis B virus core-related antigen as predicting factor for relapse after cessation of lamivudine therapy for chronic hepatitis B virus infection. Hepatol Res 2006;36:272–276.
4. Abe A, Inoue K, Tanaka T, et al. Quantitation of hepatitis B virus genomic DNA by real-time detection PCR. J Clin Microbiol 1999; 37:2899–2903.
5. Livak KJ, Schmittgen TD. Analysis of relative gene expression data using real-time quantitative PCR and the 2(-delta delta C(T)) method. Methods 2001;25:402–408.

Supplementary Table 1. Sequence of Species-Specific Primers on Fibrosis-Related Genes

Primer	Sequence
hTIMP1/F1	5′-ATGGCCCCCTTTGAGCCC-3′
hTIMP1/R1	5′-GTCTGGTTGACTTCTGGTGTC-3′
mTIMP1/F1	5′-ATGGCCCCCTTTGCATCT-3′
mTIMP1/R1	5′-GTCTCGTTGATTTCTGGGGAA-3′
hMMP2/F1	5′-CCTTCTTGTTCAATGGCAA-3′
hMMP2/R1	5′-GGACAGAAGCCGTACTTGC-3′
mMMP2/F1	5′-CCTTCCTGTTCAACGGTCG-3′
mMMP2/R1	5′-GGGCAGAAGCCATACTTGC-3′
hCOL1α2/F1	5′-AGGAAATGGCTACCCAACTT-3′
hCOL1α2/R1	5′-TTAGAGCCCTGTAGAATG-3′
mCOL1α2/F1	5′-AGGAAATGGCAACTCAGCTC-3′
mCOL1α2/R1	5′-TTGGAACCCTGCAGAAGC-3′
hGAPDH/F2	5′-CACCAGGGCTGCTTTTAACTC-3′
hGAPDH/R2	5′-AGATGGTGATGGGATTTCCA-3′
mGAPDH/F2	5′-CACCAGGGCTGCCATTTGCAG-3′
mGAPDH/R2	5′-AGATGGTGATGGGCTTCCCG-3′

COL1α2, collagen type 1α2; F, sense primer; GAPDH, glyceraldehyde-3-phosphate dehydrogenase; h, human specific; m, mouse specific; MMP2, matrix metalloproteinase 2; R, antisense primer; TIMP1, tissue inhibitor of metalloproteinase 1.

ELSEVIER

Journal of Hepatology 50 (2009) 80–88

Journal of Hepatology

www.elsevier.com/locate/jhep

Independent risk factors and predictive score for the development of hepatocellular carcinoma in chronic hepatitis B☆

Man-Fung Yuen[1,*], Yasuhito Tanaka[2], Daniel Yee-Tak Fong[3], James Fung[1], Danny Ka-Ho Wong[1], John Chi-Hang Yuen[1], David Yiu-Kuen But[1], Annie On-On Chan[1], Benjamin Chun-Yu Wong[1], Masashi Mizokami[2], Ching-Lung Lai[1]

[1]*Department of Medicine, The University of Hong Kong, Queen Mary Hospital, Pokfulam Road, Hong Kong*
[2]*Department of Clinical Molecular Informative Medicine, Nagoya City University Graduate School of Medical Sciences, Nagoya, Japan*
[3]*Department of Nursing Studies, The University of Hong Kong, Queen Mary Hospital, Hong Kong*

See Editorial, pages 7–9

***Background/Aims*: To determine whether gender, age, hepatitis B virus genotype, core promoter and precore mutations, HBeAg/anti-HBe status, HBV DNA, ALT levels and cirrhosis on presentation were independent risk factors and derive a novel risk score for the development of HCC.**

***Methods*: CHB patients (820) were followed up (mean duration 76.8 months) for the occurrence of HCC.**

***Results*: The 5- and 10-year prevalence of HCC were 4.4% and 6.3%, respectively. Cox regression analysis showed that male gender ($p = 0.025$, RR 2.98), increasing age ($p < 0.001$, RR 1.07), higher HBV DNA levels ($p = 0.02$, RR 1.28), core promoter mutations ($p = 0.007$, RR 3.66), and presence of cirrhosis ($p < 0.001$, RR 7.31) were independent risks for the development of HCC. A risk score was derived and validated with sensitivity > 84% and specificity > 76% to predict the 5- and 10-year risks for the development of HCC. The AUC for the 5- and 10-year prediction were 0.88 and 0.89, respectively.**

***Conclusions*: The risk score, based on age, gender, HBV DNA levels, core promoter mutations and cirrhosis, can estimate the chance of development of HCC in 5 and 10 years after presentation. It can be used to identify high-risk CHB patients for treatment and screening of HCC.**

***Keywords*: Chronic hepatitis B; Hepatocellular carcinoma; Risk factor; Prediction**

1. Introduction

Chronic hepatitis B (CHB) infection affects 350–400 million people worldwide [1]. These patients have a greater than 100-fold increased risk of development of hepatocellular carcinoma (HCC) compared to uninfected individuals [2]. HCC is one of the most aggressive malignancies associated with poor survival. It is very important to identify high-risk patients among carriers of CHB. This will have important implications for treatment allocation and strategic screening for HCC in CHB patients.

Received 7 April 2008; received in revised form 25 June 2008; accepted 7 July 2008; available online 21 September 2008
Associate Editor: F. Zoulim

☆ The authors declare that they do not have anything to disclose regarding funding from industries or conflict of interest with respect to this manuscript.

* Corresponding author. Tel.: +852 28553984; fax: +852 28725828.
E-mail address: mfyuen@hkucc.hku.hk (M.-F. Yuen).

Abbreviations: CHB, chronic hepatitis B; HCC, hepatocellular carcinoma; ALT, alanine aminotransferase; HBsAg, hepatitis B surface antigen; HBeAg, hepatitis B e antigen; AFP, alpha-fetoprotein; CT, computer tomography; MRI, magnetic resonance imaging; AST, aspartate aminotransferase.

0168-8278/$34.00
doi:10.1016/j.jhep.2008.07.023

Several potential factors have been identified to be associated with a higher risk of development of HCC. These include patient factors including male gender, increasing age [3]; virological factors including hepatitis B e antigen positivity, high serum HBV DNA levels, genotype C compared to B, precore mutations and core promoter mutations [4–11]; and disease factors including alanine aminotransferase (ALT) levels and presence of cirrhosis [3,12]. These risk factors are identified mostly by cross-sectional or case–cohort studies with relatively limited numbers of study population. In addition, these various listed factors may have interacting relationships. Whether these risk factors are independent factors for the development of HCC are still uncertain. A large scale, longitudinal follow-up study examining all these potential risk factors for HCC is required for more accurate assessment of prognosis in CHB patients.

We therefore conducted the present large scale longitudinal study to determine (1) the risk factors for the development of HCC, (2) which risk factors were independent risk factors for the development of HCC, and (3) whether a projected risk estimation score for the development of HCC can be derived from these independent risk factors.

2. Patients and methods

2.1. Patients

During the period between January 1995 and December 2005, all CHB patients who were first seen in our Liver Clinic, Queen Mary Hospital, Hong Kong, were followed up for the development of HCC. Patients were recruited if they were positive for hepatitis B surface antigen (HBsAg) checked by radioimmunoassay (AUSRIA II, Abbott Laboratories, North Chicago, IL) for at least 6 months and had available baseline ultrasound findings and platelet counts on presentation. Hepatitis B e antigen (HBeAg) and antibody to HBeAg (anti-HBe) were determined by the same radioimmunoassay. Patients who had HCC on presentation or other concomitant diseases including hepatitis C or D virus infection, autoimmune hepatitis, Wilson's disease, primary biliary cirrhosis, alcoholic liver disease and fatty liver (diagnosed by ultrasonography) were excluded. Patients who had received or were receiving any form of established treatment for CHB were also excluded. A total of 820 patients were recruited in the present study. Eighty-eight patients were subsequently treated for CHB. The limited number of patients receiving the treatment was due to the fact that the cost of treatment was not reimbursed in our center. Their follow-up time was censored at the time of initiation of treatment. The study was approved by the Institute Review Board of the University of Hong Kong, Hong Kong.

2.2. Monitoring of patients

Patients were followed up every 3–6 months by monitoring HBsAg status, HBeAg/anti-HBe status, liver biochemistry and alpha-fetoprotein (AFP). Ultrasound of the liver was scheduled for patients with AFP levels greater than 20 ng/mL. Computer tomography (CT) and/or magnetic resonance imaging (MRI) and/or hepatic angiogram were performed if ultrasound showed suspicion of HCC. The diagnosis of HCC was made when the patients had one of the following criteria: (1) positive histology or (2) elevated AFP levels together with imaging features compatible with HCC by CT, MRI or hepatic angiogram.

2.3. Definition of cirrhosis

Liver cirrhosis is defined by the following combined parameters: (1) score greater than 2 according to the aspartate aminotransferase (AST) to platelet ratio (APRI) using the formula: [AST/upper limit of normal]/platelet count ($\times 10^9$/L) $\times$ 100 [13], (2) ultrasonographic evidence of small sized liver with and without splenomegaly/ascites, and (3) albumin level less than 35 g/L without other identifiable causes of hypoalbuminemia such as renal loss or gastrointestinal loss.

2.4. Determination of HBV genotypes, core promoter/precore mutations and HBV DNA levels

Sera from patients on presentation were taken for the following tests: (1) HBV genotyping performed by an enzyme-linked immunosorbent assay (ELISA) as described in a previous study [14], (2) core promoter (A1762T/G1764A) and precore (G1896A) mutations determined by direct sequencing described in another study [15], (3) HBV DNA levels determined by the Cobas Amplicor HBV Monitor test, Roche Diagnostics, Branchburg, NJ, with the lower limit of detection of 300 copies/mL. HBV DNA levels below the lower detection limit were regarded as 300 copies/mL for statistical calculations.

2.5. Statistical analysis

Statistical analyses to identify risk factors were performed using the SPSS 14.0 for Windows, SPSS Inc., Chicago, IL). Mann–Whitney U test was used to compare continuous variables with skew distribution. Kaplan–Meier analysis using log rank test was used to compare the cumulative risks of development of HCC in different groups of patients. Cox regression analysis was used to determine whether the identified variables associated with HCC were independent risk factors.

Statistical analyses to formulate a risk score for the development of HCC were performed by using the R 2.4.1 version (A language and environment for statistical computing, Vienna, Austria, ISBN 3-900051-07-0, URL http://www.R-project.org). This score was constructed as a weighted sum of sex, age, HBV DNA levels in copies/mL in log, cirrhosis, and core promoter mutations. The weights were taken as the corresponding estimated coefficients in a Cox regression analysis after divided by the smallest coefficient and rounded to the nearest integer.

The accuracy of using the derived HCC score for predicting the development of HCC at 5 and 10 years after presentation was examined by first estimating a time-dependent Receiver Operating Characteristic curve by the Nearest Neighbor Estimation method [16]. The area under curve (AUC) was then calculated for measuring the overall prediction accuracy. A 95% confidence interval for an AUC was obtained by sampling the 820 patients for 1000 bootstrap samples with the confidence limits calculated as the 2.5th and 97.5th percentiles. The score was assessed by the leave-one-out cross-validation in order to assess the performance of the HCC score in new data [17]. Specifically, the first of the 820 patients was dropped before we re-did the determination of the weights for calculating a risk score. The weights were used to calculate the score for the first patient. Similarly, the second patient was dropped before its score was calculated based on the other 819 patients. The process continued until all patients had their score calculated.

To ease clinical application of the risk score, cut-off values for the prediction of HCC development at 5 and 10 years were determined by maximizing the Youden index, i.e. sensitivity + specificity − 1, calculated from the time-dependent ROC analysis. Accuracy of using the optimal cut-off values was assessed by the sensitivity, specificity, predictive values and likelihood ratios. Their

Table 1
Baseline demographic and virological data of the study population

Number of patients	820
Sex (M:F)	573:247
Age (years)	40.6 (13.5–83.2)
HBeAg/anti-HBe	356:464 (43.4%:56.6%)
Albumin (g/L)	44 (22–56)
Bilirubin (μmol/L)	11 (1–77)
Alanine aminotransferase (U/L)	47 (5–1251)
Platelet count ($\times 10^9$)/L	175 (55–290)
HBV DNA (log copies/mL)	6.01 (2.5–13)
Genotype (B:C)	328:492 (40%:60%)
Core promoter mutations, WT: MT	312:508 (38%:62%)
Precore mutations, WT:MT	502:318 (61.2%:38.8%)
Cirrhosis	124 (15.1%)

Continuous variables are expressed in median (range). WT, wild-type; MT, mutant.

95% confidence intervals were again obtained by 1000 bootstrap samples. The cut-off values were also cross-validated by the leave-one-out method.

3. Results

3.1. Demographics

A total of 820 CHB patients were recruited. The baseline demographics, liver function tests, platelet counts and virological data are listed in Table 1. The mean and median follow-up duration were 76.8 months (standard deviation 36.2) and 67.4 months (range 6.4–221.4), respectively.

3.2. Characteristics of patients with HCC

Forty (4.9%) patients developed HCC. Thirty-five (87.5%) patients were male. The median age of development of HCC was 57.3 years (range 24.9–84.2). At the time of development of HCC, 12 (30%) patients were HBeAg positive and 24 (70%) were anti-HBe positive (5 were HBeAg positive on presentation and underwent HBeAg seroconversion on subsequent follow-up).

3.3. Patients' factors for the development of HCC

Male patients had a higher cumulative risk of development of HCC compared to female patients (Fig. 1, $p = 0.01$). The median age on presentation of patients with HCC was significantly older compared to that of patients without HCC [54.2 years (range 19.4–81.7) vs. 39.8 years (range 13.5–83.2), respectively, $p < 0.001$].

3.4. Virological factors for the development of HCC

There was no significant difference in the cumulative risk of development of HCC between patients with HBV genotype B and C (Fig. 2, $p = 0.26$) and between patients with precore mutations and wild-type (Fig. 2, $p = 0.64$). However, patients with core promoter mutations had a significantly higher cumulative risk of development of HCC compared to patients with core promoter wild-type (Fig. 2, $p < 0.001$). There was a stepwise increase in the cumulative risks of HCC with increasing levels of HBV DNA in log copies/mL starting from HBV DNA levels of $\geqslant 4$ logs (Fig. 3, $p = 0.028$).

For the HBeAg/anti-HBe status on presentation, there was no difference in the cumulative risk of HCC between patients who were positive for HBeAg ($n = 356$) and positive for anti-HBe ($n = 464$) on presentation ($p = 0.54$). Since 144 out of 356 HBeAg-positive

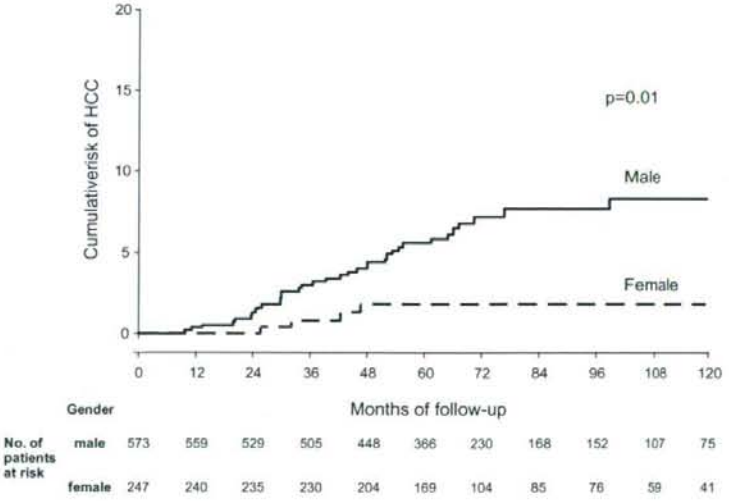

Fig. 1. Cumulative risks for the development of hepatocellular carcinoma in male and female patients.

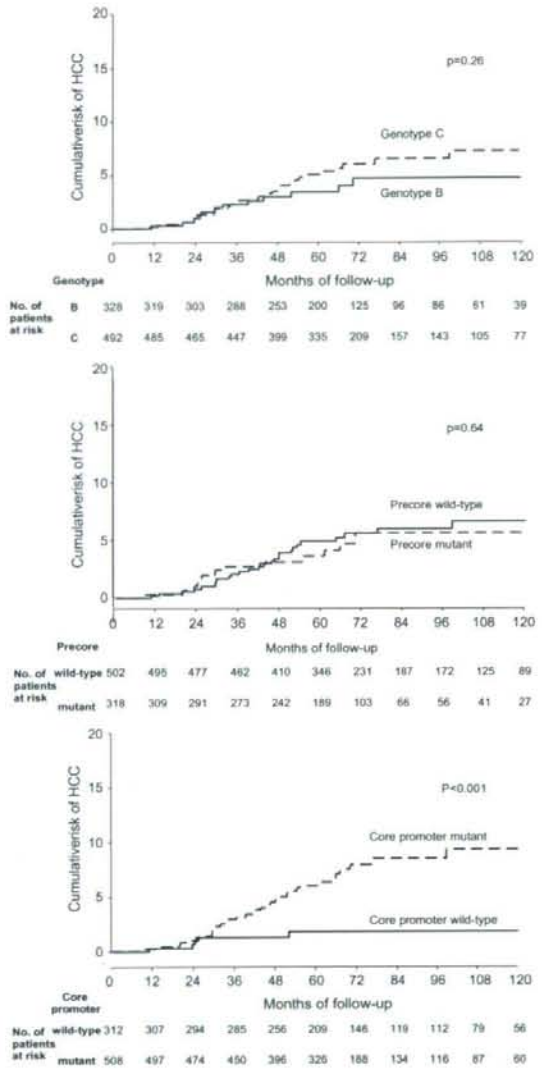

Fig. 2. Cumulative risks for the development of hepatocellular carcinoma in patients with genotype B and C (upper diagram), with precore mutant and wild-type (middle diagram), and with core promoter mutant and wild-type (lower diagram).

patients underwent subsequent HBeAg seroconversion to anti-HBe, patients are further classified into group 1 (persistent HBeAg positivity), group 2 (HBeAg positivity on presentation and with HBeAg seroconversion to anti-HBe during subsequent follow-up) and group 3 (persistent anti-HBe positivity). There were again no differences in the cumulative risk of development of HCC between these 3 groups of patients (Fig. 4, $p = 0.22$ for group 1 vs. group 2; $p = 0.94$ for group 1 vs. group 3; $p = 0.24$ for group 2 vs. group 3).

3.5. Disease factors for the development of HCC

Patients were stratified into 3 groups according to ALT levels on presentation [ALT < 0.5 upper limit of normal (ULN) vs. 0.5–1 × ULN vs. >1 × ULN]. Patients with ALT levels <0.5 × ULN had a significantly lower cumulative risk of development of HCC compared to patients with ALT levels between 0.5–1 × ULN ($p = 0.008$) and >1 × ULN ($p = 0.007$) (Fig. 5). There was no difference in the cumulative risk for the development of HCC between the latter two groups ($p = 0.95$).

Patients with pre-existing cirrhosis had a significantly higher cumulative risk of development of HCC compared to patients without cirrhosis (Fig. 5, $p < 0.001$).

3.6. Multivariate analysis for factors associated with development of HCC

Univariate analyses showed that male gender, increasing age, higher HBV DNA levels in log copies/mL, presence of core promoter mutations, ALT levels higher than 0.5 × ULN and presence of pre-existing cirrhosis were significant risk factors for the development of HCC. On further calculation using Cox Regression analysis, the followings were found to be independent risk factors for the development to HCC: male gender [$p = 0.025$, relative risk (RR) 2.98 [95% confidence interval (CI) 1.15–7.78]; increasing age ($p < 0.001$, RR 1.07, 95% CI 1.04–1.09); higher HBV DNA levels in log copies/ml ($p = 0.02$, RR 1.28, 95% CI 1.04–1.58); core promoter mutations ($p = 0.007$, RR 3.66, 95% CI 1.42–9.47); and presence of cirrhosis ($p < 0.001$, RR 7.31, 95% CI 3.76–14.21). ALT level was not an independent factor ($p = 0.35$).

3.7. Predictive score for the development of HCC

The 5-year and 10-year prevalence of HCC were 4.4% (95% CI 2.9–5.9%) and 6.3% (95% CI 4.2–8.3%). The derived HCC score was formulated as *16 * sex (male = 1; female = 0) + age (in years) + 3 * HBV DNA levels (copies/mL in log) + 19 * core promoter mutations (mutant = 1; wild-type = 0) + 30 * cirrhosis (presence = 1; absence = 0)*. This score is abbreviated as "GAG-HCC" score from "Guide with Age, Gender, HBV DNA, Core promoter mutations and Cirrhosis". The hazard ratio of GAG-HCC score for the development of HCC was 1.07 (95% CI 1.05–1.08, $p < 0.001$) indicating that the risk of development of HCC increased by 7% with an increase of score value by one. The hazard ratio of the score by the leave-one-out cross-validation was 1.06 (95% CI 1.05–1.08, $p < 0.001$). By optimizing with the Youden's index, the optimal cut-off of the HCC score for the prediction of 5- and 10-year development of HCC was

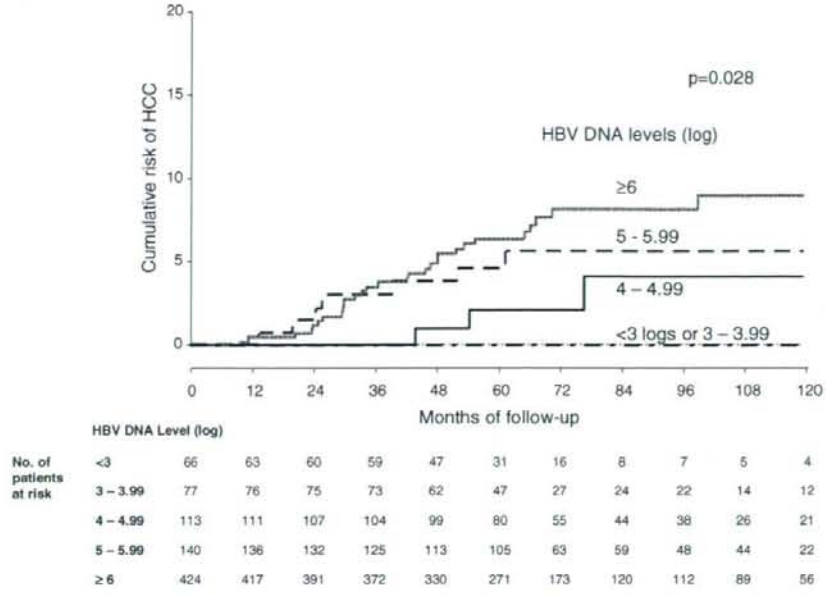

HBV DNA Level (log)											
No. of patients at risk	<3	66	63	60	59	47	31	16	8	7	5	4
	3 – 3.99	77	76	75	73	62	47	27	24	22	14	12
	4 – 4.99	113	111	107	104	99	80	55	44	38	26	21
	5 – 5.99	140	136	132	125	113	105	63	59	48	44	22
	≥ 6	424	417	391	372	330	271	173	120	112	89	56

Fig. 3. Cumulative risks for the development of hepatocellular carcinoma in patients with different HBV DNA levels (copies/mL) in log.

101. This cut-off had good sensitivity and specificity and had been accurately validated by the leave-one-out-validation (Table 2). The AUCs were as high as 0.88 (95% CI 0.82–0.93) and 0.89 (95% CI 0.85–0.93) for 5- and 10-year prediction, respectively. The estimated chances of development of HCC at 5 and 10 years according to the score on presentation are depicted in Fig. 6.

Since the data on core promoter mutations may not be easily available in some centers, the score was formulated again without incorporating core promoter mutations to predict the 5- and 10-year risk of development of HCC. Using the same statistical methodology, the risk score was *14 * sex (male = 1; female = 0) + age (in years) + 3 * HBV DNA levels (copies/mL in log) + 33 * cirrhosis (presence = 1; absence = 0)*. The

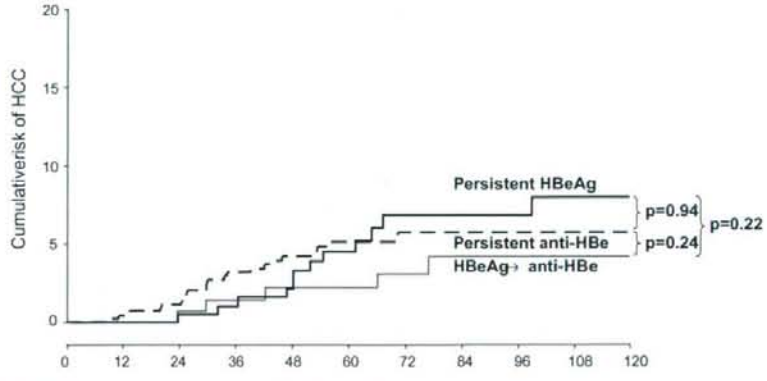

HBeAg/ anti-HBe status											
No. of patients at risk	persistent HBeAg	212	197	197	187	169	142	98	88	83	53	35
	HBeAg →anti-HBe	144	142	139	136	125	115	92	87	83	67	51
	persistent anti-HBe	464	450	432	412	358	278	144	78	62	46	30

Fig. 4. Cumulative risks for the development of hepatocellular carcinoma in patients with persistently positive HBeAg, HBeAg seroconversion to anti-HBe and persistently positive anti-HBe.

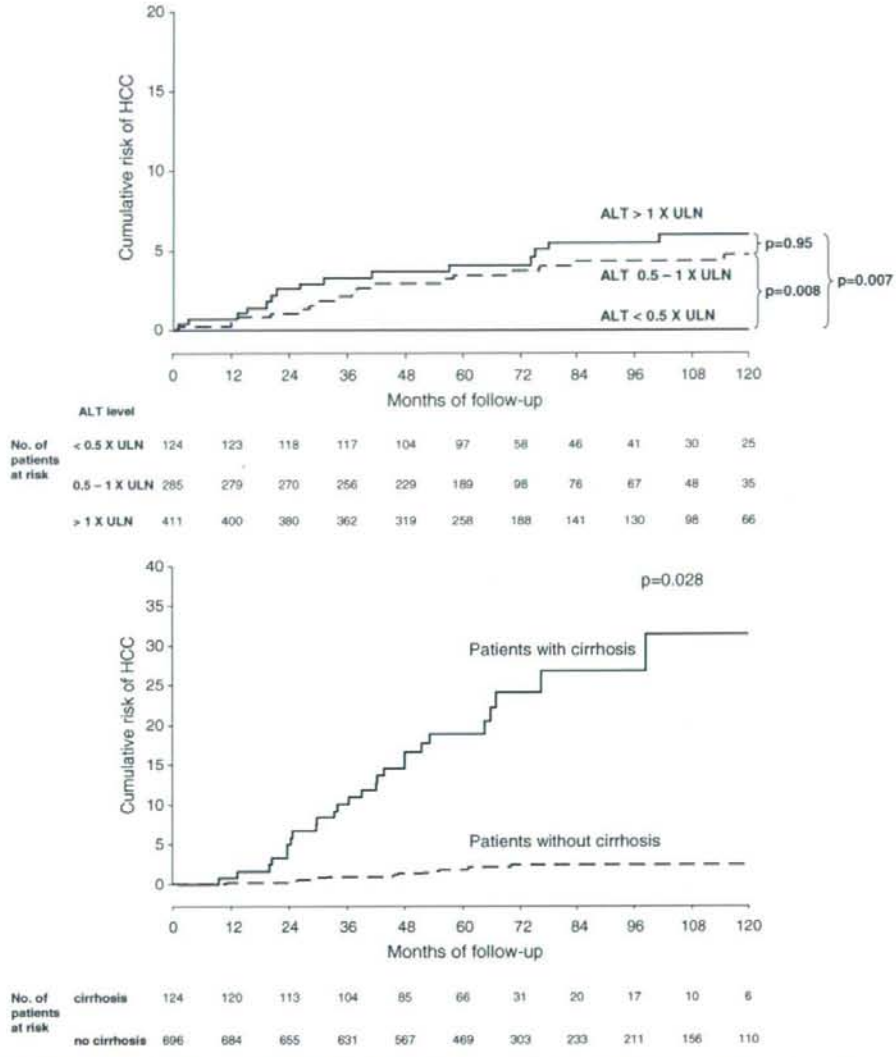

Fig. 5. Cumulative risks for the development of hepatocellular carcinoma in patients with different levels of alanine aminotransferase (upper diagram) and in patients with and without cirrhosis (lower diagram).

hazard ratio of this score without core promoter mutations was 1.06 (95% CI 1.05–1.08, $p < 0.001$). The hazard ratio of this score by the leave-one-out cross-validation was 1.06 (95% CI 1.05–1.08, $p < 0.001$). By optimizing with the Youden's index, the optimal cut-off of the HCC score without core promoter mutations for the prediction of 5- and 10-year development of HCC were 100 and 82, respectively. The sensitivity and specificity of these cut-off values are listed in Table 3. The AUCs were 0.87 (95% CI 0.82–0.93) and 0.88 (95% CI 0.82–0.92) for 5- and 10-year prediction, respectively. The estimated chances of development of HCC at 5 and 10 years according to the score without core promoter mutations on presentation are shown in Fig. 6.

4. Discussion

There are two main unsettling issues concerning study reliability and utility of the clinical risk factors for the development of HCC. First, risk factors may be inter-related or inter-dependent and thus confound the calculation of risk development. Second, when there is more than one risk factor for the development of HCC, the risk estimations are not simply additive. It

Table 2
Optimal cut-off values by maximizing Youden index and their accuracies for the HCC score derived from whole study population and validated with leave-one-out cross-validation

	5-year prediction		10 year prediction	
	Value	95% CI	Value	95% CI
Total study population				
Optimal cut-off	101		101	
Sensitivity	84.1%	(67.7%, 97.5%)	88.0%	(76.7%, 95.3%)
Specificity	76.2%	(60.8%, 90.7%)	78.7%	(73.8%, 87.7%)
Positive predictive value	14.0%	(10.0%, 26.3%)	21.7%	(18.0%, 32.9%)
Negative predictive value	98.3%	(99.5%, 99.9%)	99.0%	(98.0%, 99.6%)
Positive likelihood ratio	3.54	(2.38, 7.81)	4.13	(3.27, 7.10)
Negative likelihood ratio	0.21	(0.04, 0.38)	0.15	(0.06, 0.29)
Leave-one-out cross-validation				
Optimal cut-off	101		101	
Sensitivity	87.9%	(74.0%, 100%)	100%	(76.9%, 100%)
Specificity	76.2%	(73.3%, 79.1%)	79.1%	(75.3%, 83.5%)
Positive predictive value	14.6%	(12.2%, 17.2%)	25.7%	(18.1%, 35.6%)
Negative predictive value	99.3%	(98.4%, 100%)	100%	(98.0%, 100%)
Positive likelihood ratio	3.70	(3.02, 4.50)	5.18	(3.31, 8.25)
Negative likelihood ratio	0.16	(0, 0.34)	0	(0, 0.30)

has been shown that the risk for the development of HCC increases dramatically when two risk factors are present concomitantly [18]. This makes simple risk stratification for CHB patients very difficult. The present study tackled these difficulties. One of the limitations of the present study is the possibility of underestimation of the rate of development of HCC since abdominal ultrasound was performed only when patients had elevated AFP levels. Another limitation was that the definition of cirrhosis was not reached from liver biopsies. This may lead to an underestimation of subclinical cirrhosis of the study population. However using our criteria, which were easily available in clinical practice, patients with frank cirrhosis could be identified with reasonable accuracy. In addition, our criteria may be much easier to apply in clinical practice compared to adopting histological assessment for cirrhosis, thus reinforcing the usefulness of the proposed score.

In line with several studies [19,20], HBV genotypes B and C did not differ in the risk for development of HCC. The apparent association between genotype C and HCC reported in some studies [21–23] may be related to the close connection between genotype C and core promoter mutations [24]. In contrast, the presence of core promoter mutations was an independent risk factor for the development of HCC. This is in accordance with previous studies [9–11,18,25,26]. Two previous studies

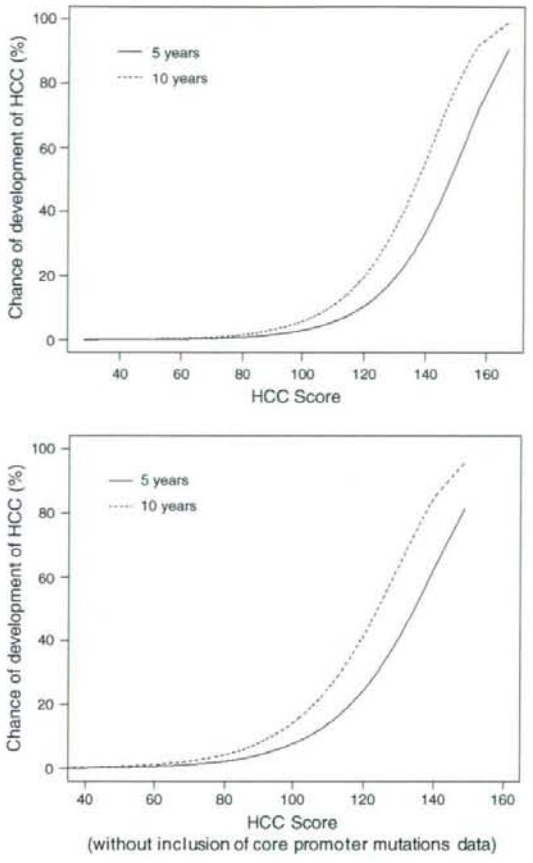

Fig. 6. Chance of the development of hepatocellular carcinoma at 5 and 10 years according to the different values of the HCC score on presentation using the GAG-HCC score (upper diagram) and the score without inclusion of the data of core promoter mutations (lower diagram).

showed that patients with core promoter mutations have higher HBV DNA levels compared to patients without core promoter mutations [27,28].

Apart from core promoter mutations, the present study also found that increasing HBV DNA levels from 4 to >6 logs copies/mL were independently associated with a stepwise increase in the risk for the development of HCC. Importantly, HBeAg and anti-HBe status were not risk factors for the development of HCC. This is true for both the HBeAg/anti-HBe status on presentation and during subsequent follow-up. Our findings that HBV DNA levels and not HBeAg/anti-HBe status were risk factors for the development of HCC are similar to the conclusion of a large scale study from Taiwan (The REVEAL study) [5]. This has obvious implication on whether HBeAg seroconversion *alone* is an adequate endpoint for treatment of HBeAg-positive patients.

Table 3
Optimal cut-off values by maximizing Youden index and their accuracies for the HCC score *without inclusion of the data of core promoter mutations* derived from whole study population and validated with leave-one-out cross-validation

	5-year prediction		10 year prediction	
	Value	95% CI	Value	95% CI
Total study population				
Optimal cut-off	100		82	
Sensitivity	67.8%	(62.4%, 99.3%)	86.6%	(69.7%, 96.3%)
Specificity	88.1%	(59.0%, 91.5%)	75.6%	(65.5%, 90.3%)
Positive predictive value	20.9%	(9.4%, 27.9%)	19.2%	(14.6%, 34.5%)
Negative predictive value	98.3%	(98.1%, 99.9%)	98.8%	(97.7%, 99.7%)
Positive likelihood ratio	5.72	(2.24, 8.37)	3.55	(2.56, 7.88)
Negative likelihood ratio	0.37	(0.01, 0.43)	0.18	(0.05, 0.35)
Leave-one-out cross-validation				
Optimal cut-off	100		82	
Sensitivity	69.6%	(51.1%, 86.7%)	100%	(74.9%, 100%)
Specificity	87.9%	(85.4%, 90.2%)	75.3%	(71.4%, 79.2%)
Positive predictive value	21.0%	(15.5%, 26.6%)	21.7%	(15.8%, 28.4%)
Negative predictive value	98.4%	(97.5%, 99.3%)	100%	(97.8%, 100%)
Positive likelihood ratio	5.75	(3.96, 7.86)	4.14	(2.80, 5.93)
Negative likelihood ratio	0.35	(0.15, 0.56)	0	(0, 0.34)

The present study confirmed that presence of cirrhosis at baseline was the most important independent risk factor because its relative risk for development of HCC for patients with cirrhosis was the highest among the five independent risk factors (male gender, increasing age, HBV DNA level, core promoter mutations and cirrhosis). Another virological factor, namely preS deletion has not been examined in the study population. It has been recently documented to be an important risk factor for the development of HCC [29]. The predictive power of scoring system for the development of HCC may be augmented if preS deletion can also be incorporated in the model in the future studies.

After identifying these five independent risk factors for the development of HCC, the present study derived a novel "GAG-HCC" score which was able to identify patients who were at risk of development of HCC if the score was greater or equal to the optimal cut-off value of 101. This score was validated by the stringent leave-one-out statistical analysis with high sensitivity and specificity of 88.0% and 78.7% for the prediction at 10 years, respectively. The chance of development of HCC increased exponentially once the score was $\geqslant 101$ (Fig. 6). There is a slight decrease in the sensitivity (86.6%) and specificity (75.6%) for the 10 year prediction by using the score without inclusion of the data of core promoter mutations (Table 3). Using these risk scores, one can calculate the prognosis of patients on presentation which is important for a clinician in devising each individual patient's management. One can also identify very high-risk patients (e.g. $\geqslant 50\%$ chance of developing HCC in 5 years and 10 years if the GAG-HCC score were $\geqslant 148$ and 136, respectively) who should be strongly recommended for treatment by nucleoside/nucleotide analogues to lower one of the two remediable/preventable factors in the score, the HBV DNA levels. Treatment with nucleoside/nucleotide analogues can also potentially prevent or delay the development of cirrhosis (another remediable/preventable risk factor). Even for patients with established cirrhosis, nucleoside/nucleoside analogues have been shown to potentially revert it [30].

In clinical practice, we are not aware of any predictive score for the development of HCC in CHB patients with the integration of all possible independent factors. Our novel score may serve as a good reference for clinicians to decide who should have regular screening for HCC and who should be treated preferentially. It has been shown that early detection of HCC by screening is associated with a higher chance of receiving more curative treatment [31].

In conclusion, male gender, increasing age, HBV DNA levels, presence of core promoter mutations and cirrhosis on presentation are independently associated with development of HCC in CHB patients. A novel GAG-HCC score has been formulated. It is of great clinical use to identify CHB patients at high-risk for the development of HCC. These patients should be treated by drugs to lower the HBV DNA levels and carefully monitored for the development of HCC.

References

[1] Lee WM. Hepatitis B virus infection. N Engl J Med 1997;337:1733–1745.
[2] Beasley RP, Hwang LY, Lin CC, Chien CS. Hepatocellular carcinoma and hepatitis B virus. A prospective study of 22707 men in Taiwan. Lancet 1981;2:1129–1133.
[3] Sherman M. Hepatocellular carcinoma: epidemiology, risk factors, and screening. Semin Liver Dis 2005;25:143–154.
[4] Yang HI, Lu SN, Liaw YF, You SL, Sun CA, Wang LY, et al. Hepatitis B e antigen and the risk of hepatocellular carcinoma. N Engl J Med 2002;347:168–174.
[5] Chen CJ, Yang HI, Su J, Jen CL, You SL, Lu SN, et al. Risk of hepatocellular carcinoma across a biological gradient of serum hepatitis B virus DNA level. JAMA 2006;295:65–73.
[6] Tsubota A, Arase Y, Ren F, Tanaka H, Ikeda K, Kumada H. Genotype may correlate with liver carcinogenesis and tumor characteristics in cirrhotic patients infected with hepatitis B virus subtype adw. J Med Virol 2001;65:257–265.
[7] Chan HL, Hui AY, Wong ML, Tse AM, Hung LC, Wong VW, et al. Genotype C hepatitis B virus infection is associated with an increased risk of hepatocellular carcinoma. Gut 2004;53:1494–1498.

[8] Tong MJ, Blatt LM, Kao JH, Cheng JT, Corey WG. Precore/basal core promoter mutants and hepatitis B viral DNA levels as predictors for liver deaths and hepatocellular carcinoma. World J Gastroenterol 2006;12:6620–6626.
[9] Baptista M, Kramvis A, Kew MC. High prevalence of 1762(T) 1764(A) mutations in the basic core promoter of hepatitis B virus isolated from black Africans with hepatocellular carcinoma compared with asymptomatic carriers. Hepatology 1999;29:946–953.
[10] Kao JH, Chen PJ, Lai MY, Chen DS. Basal core promoter mutations of hepatitis B virus increase the risk of hepatocellular carcinoma in hepatitis B carriers. Gastroenterology 2003;124:327–334.
[11] Liu CJ, Chen BF, Chen PJ, Lai MY, Huang WL, Kao JH, et al. Role of hepatitis B viral load and basal core promoter mutation in hepatocellular carcinoma in hepatitis B carriers. J Infect Dis 2006;193:1258–1265.
[12] Yuen MF, Yuan HJ, Wong DK, Yuen JC, Wong WM, Chan AO, et al. Prognostic determinants for chronic hepatitis B in Asians: therapeutic implications. Gut 2005;54:1610–1614.
[13] Wai CT, Greenson JK, Fontana RJ, Kalbfleisch JD, Marrero JS, Conjeevaram HS, et al. A simple noninvasive index can predict both significant fibrosis and cirrhosis in patients with chronic hepatitis C. Hepatology 2003;38:518–526.
[14] Sugauchi F, Orito E, Ichida T, Kato H, Sakugawa H, Kakumu S, et al. Epidemiologic and virologic characteristics of hepatitis B virus genotype B having the recombination with genotype C. Gastroenterology 2003;124:925–932.
[15] Yuen MF, Tanaka Y, Mizokami M, Yuen JC, Wong DK, Yuan HJ, et al. Role of hepatitis B virus genotypes Ba and C, core promoter and precore mutations on hepatocellular carcinoma: a case control study. Carcinogenesis 2004;25:1593–1598.
[16] Heagerty PJ, Lumley T, Pepe MS. Time-dependent ROC curves for censored survival data and a diagnostic marker. Biometrics 2000;56:337–344.
[17] Hastie T, Tibshirani R, Friedman J. The elements of statistical learning. 1st ed. New York: Springer; 2001, p. 214–7.
[18] Yuen MF, Tanaka Y, Shinkai N, Poon RT, But DY, Fong DY, et al. Risk for hepatocellular carcinoma with respect to hepatitis B virus genotypes B/C, specific mutations of enhancer II/core promoter/precore regions and HBV DNA levels. Gut 2008;57:98–102.
[19] Yuen MF, Sablon E, Yuan HJ, Wong DK, Hui CK, Wong BC, et al. Significance of hepatitis B genotype in acute exacerbation, HBeAg seroconversion, cirrhosis-related complications, and hepatocellular carcinoma. Hepatology 2003;37:562–567.
[20] Sumi H, Yokosuka O, Seki N, Arai M, Imazeki F, Kurihara T, et al. Influence of hepatitis B virus genotypes on the progression of chronic type B liver disease. Hepatology 2003;37:19–26.
[21] Fujie H, Moriya K, Shintani Y, Yotsuyanagi H, Iino S, Koike K. Hepatitis B virus genotypes and hepatocellular carcinoma in Japan. Gastroenterology 2001;120:1564–1565.
[22] Sakugawa H, Nakasone H, Nakayoshi T, Orito E, Mizokami M, Yamashiro T, et al. Preponderance of hepatitis B virus genotype B contributes to a better prognosis of chronic HBV infection in Okinawa, Japan. J Med Virol 2002;67:484–489.
[23] Orito E, Mizokami M, Sakugawa H, Michitaka K, Ishikawa K, Ichida T, et al. A case–control study for clinical and molecular biological differences between hepatitis B viruses of genotypes B and C. Hepatology 2001;33:218–223.
[24] Yuen MF, Sablon E, Tanaka Y, Kato T, Mizokami M, Doutreloigne J, et al. Epidemiological study of hepatitis B virus genotypes, core promoter and precore mutations of chronic hepatitis B infection in Hong Kong. J Hepatol 2004;41:119–125.
[25] Liu CJ, Chen BF, Chen PJ, Lai MY, Huang WL, Kao JH, et al. Role of hepatitis B virus precore/core promoter mutations and serum viral load on noncirrhotic hepatocellular carcinoma: a case–control study. J Infect Dis 2006;194:594–599.
[26] Chou YC, Yu MW, Wu CF, Yang SY, Lin CL, Liu CJ, et al. Temporal relationship between hepatitis B virus enhancer II/basal core promoter sequence variation and risk of hepatocellular carcinoma. Gut 2008;57:91–97.
[27] Chauhan R, Kazim SN, Bhattacharjee J, Sakhuja P, Sarin SK. Basal core promoter, precore region mutations of HBV and their association with e antigen, genotype, and severity of liver disease in patients with chronic hepatitis B in India. J Med Virol 2006;78:1047–1054.
[28] Pang A, Yuen MF, Yuan HJ, Lai CL, Kwong YL. Real-time quantification of hepatitis B virus core-promoter and pre-core mutants during hepatitis E antigen seroconversion. J Hepatol 2004;40:1008–1017.
[29] Lin CL, Liu CH, Chen W, Huang WL, Chen PJ, Lai MY, et al. Association of pre-S deletion mutant of hepatitis B virus with risk of hepatocellular carcinoma. J Gastroenterol Hepatol 2007;22:1098–1103.
[30] Dienstag JL, Goldin RD, Heathcote EJ, Hann HW, Woessner M, Stephenson SL, et al. Histological outcome during long-term lamivudine therapy. Gastroenterology 2003;124:105–117.
[31] Yuen MF, Cheng CC, Lauder IJ, Lam SK, Ooi CG, Lai CL. Early detection of hepatocellular carcinoma increases the chance of treatment: Hong Kong experience. Hepatology 2000;31:330–335.

JOURNAL OF VIROLOGY, June 2008, p. 5715–5724 Vol. 82, No. 12
0022-538X/08/$08.00+0 doi:10.1128/JVI.02530-07

Critical Role of Virion-Associated Cholesterol and Sphingolipid in Hepatitis C Virus Infection▽

Hideki Aizaki,[1] Kenichi Morikawa,[1] Masayoshi Fukasawa,[2] Hiromichi Hara,[1] Yasushi Inoue,[1] Hideki Tani,[3] Kyoko Saito,[2] Masahiro Nishijima,[2] Kentaro Hanada,[2] Yoshiharu Matsuura,[3] Michael M. C. Lai,[4] Tatsuo Miyamura,[1] Takaji Wakita,[1] and Tetsuro Suzuki[1]*

Department of Virology II[1] and Department of Biochemistry and Cell Biology,[2] National Institute of Infectious Diseases, Tokyo 162-8640, and Department of Molecular Virology, Research Institute for Microbial Diseases, Osaka University, Osaka 565-0871,[3] Japan, and Department of Molecular Microbiology and Immunology, University of Southern California, Los Angeles, California 90033-1054[4]

Received 27 November 2007/Accepted 17 March 2008

In this study, we establish that cholesterol and sphingolipid associated with hepatitis C virus (HCV) particles are important for virion maturation and infectivity. In a recently developed culture system enabling study of the complete life cycle of HCV, mature virions were enriched with cholesterol as assessed by the molar ratio of cholesterol to phospholipid in virion and cell membranes. Depletion of cholesterol from the virus or hydrolysis of virion-associated sphingomyelin almost completely abolished HCV infectivity. Supplementation of cholesterol-depleted virus with exogenous cholesterol enhanced infectivity to a level equivalent to that of the untreated control. Cholesterol-depleted or sphingomyelin-hydrolyzed virus had markedly defective internalization, but no influence on cell attachment was observed. Significant portions of HCV structural proteins partitioned into cellular detergent-resistant, lipid-raft-like membranes. Combined with the observation that inhibitors of the sphingolipid biosynthetic pathway block virion production, but not RNA accumulation, in a JFH-1 isolate, our findings suggest that alteration of the lipid composition of HCV particles might be a useful approach in the design of anti-HCV therapy.

Hepatitis C virus (HCV) is recognized as a major cause of chronic liver disease, including chronic hepatitis, hepatic steatosis, cirrhosis, and hepatocellular carcinoma. It presently affects approximately 200 million people worldwide (26). HCV is an enveloped positive-strand RNA virus belonging to the *Hepacivirus* genus of the family *Flaviviridae*. Its genome of ~9.6 kb encodes a polyprotein precursor of ~3,000 residues, and the structural proteins (core, E1, and E2) reside in its N-terminal region.

Little is known about the assembly of HCV and its virion structure, because efficient production of authentic HCV particles has only recently been achieved. Nucleocapsid assembly generally involves oligomerization of the capsid protein and encapsidation of genomic RNA. This process is thought to occur upon interaction of the core protein with viral RNA, and this core-RNA interaction may induce a change from RNA replication to packaging. As with related viruses, the mature HCV virion likely consists of a nucleocapsid and an outer envelope composed of a lipid membrane and envelope proteins. Expression of the structural proteins in mammalian cells has been observed to generate virus-like particles with ultrastructural properties similar to those of HCV virions (5, 29). Packaging of these HCV-like particles into intracellular vesicles as a result of budding from the endoplasmic reticulum (ER) has also been observed (8, 34). However, HCV structural proteins are observed both in the ER and in the Golgi apparatus (45). Moreover, complex N-linked glycans have been detected on the surfaces of HCV particles isolated from patient sera, suggesting that the glycans transit through the Golgi apparatus (44). Interactions between the core and E1/E2 proteins are thought to determine viral morphology and are mediated through a cytoplasmic loop present in the polytopic form of E1 (35). Recently, we and others have identified a unique HCV genotype 2a isolate, JFH-1, that is able to replicate and produce high levels of infectious virus in culture (HCVcc) (54, 56), enabling us to investigate new aspects of the HCV life cycle.

In this study, we examine the importance of cholesterol and sphingolipid in association with the HCV membrane in virion maturation and virus infectivity. Mature HCV particles are rich in cholesterol. Cholesterol depletion or hydrolysis of sphingolipid from HCV particles results in a loss of infectivity. We further demonstrate a requirement for virion-associated cholesterol and sphingolipid for viral entry.

MATERIALS AND METHODS

Cell culture. The human hepatoma cell line Huh-7, which is permissive to HCV infection, was obtained from Francis V. Chisari (The Scripps Research Institute). Human embryonic kidney 293T cells were cultured in Dulbecco's modified Eagle medium (DMEM)–10% fetal bovine serum. Huh-7 cell lines, which carry subgenomic replicon RNA of either the JFH-1 (20) or the N (11, 17) strain, were cultured as previously described (21, 46).

Reagents. The primary antibodies used in this study were mouse monoclonal antibodies against vesicular stomatitis virus glycoprotein (VSV-G) (Sigma, St. Louis, MO), HCV E1 (54) and E2 (Biodesign International, Saco, ME), caveolin-2 (New England Biolabs, Beverly, MA), and CD81 (BD Pharmingen, Franklin Lakes, NJ), as well as rabbit polyclonal antibodies against calnexin (Stressgen, Ann Arbor, MI) and HCV core (48). ISP-1/myriocin, cholesterol, and

* Corresponding author. Mailing address: Department of Virology II, National Institute of Infectious Diseases, 1-23-1 Toyama, Shinjuku-ku, Tokyo 162-8640, Japan. Phone: 81 3 5285 1111. Fax: 81 3 5285 1161. E-mail: tesuzuki@nih.go.jp.

▽ Published ahead of print on 26 March 2008.

heparinase I were purchased from Sigma, and recombinant *Bacillus cereus* sphingomyelinase (SMase) was obtained from Higeta Shoyu (Tokyo, Japan). (1*R*,3*R*)-*N*-(3-Hydroxy-1-hydroxymethyl-3-phenylpropyl) dodecanamide (HPA-12), which was synthesized as described elsewhere (24), was a gift from Shu Kobayashi (University of Tokyo).

Plasmids. pCAE1 and pCAE2 contain HCV cDNAs spanning the E1 region (amino acids 192 to 383) with a FLAG tag at the N terminus and the E2 region (amino acids 384 to 809) with a Myc tag at the N terminus of strain NIHJ1 (1), respectively, under the control of the CAG promoter (38). pCAV340V and pCAV711V consist of the ectodomains of E1 and E2, respectively, with the N-terminal signal sequences, transmembrane domains, and cytoplasmic domains derived from VSV-G, as described elsewhere (50) (see Fig. 4D).

Virus production. Plasmid pJFH1, containing full-length cDNA of the JFH-1 isolate, was used to generate HCVcc as described elsewhere (23, 33, 34, 54). pJ6/JFH was obtained from JFH1 by replacement of the 5′ untranslated region to the p7 region (EcoRI-BclI) of J6. In vitro-transcribed RNA from linearized pJFH1 or pJ6/JFH1 was delivered to Huh-7 cells by electroporation. Culture supernatants were collected at 72 h posttransfection, clarified by low-speed centrifugation, passed through a 0.45-mm-pore-size filter, and concentrated using an Amicon Ultra-15 unit (Millipore, Bedford, MA) or by ultracentrifugation (23). Infectious titers, HCV RNA copies, and core protein concentrations of the viral stocks were $\sim 5 \times 10^5$ focus-forming units per ml, $\sim 1 \times 10^7$ copies/ml, and $\sim 1 \times 10^4$ fmol/liter, respectively. HCVcc was isolated by a combination of ultrafiltration, ion-exchange chromatography, heparin affinity chromatography, and sucrose density ultracentrifugation (33; K. Morikawa and T. Wakita, unpublished data). Pseudotyped VSV containing E1 and E2 proteins of the HCV genotype 1a isolate H77c (HCVpv) was generated as previously described (51). Briefly, 293T cells transiently expressing E1 and E2 proteins (strain H77) were infected with VSVdelG-GFP/G, in which the G envelope gene was replaced with green fluorescent protein (GFP) and pseudotyped with VSV-G.

Determination of cholesterol and phospholipid contents of HCVcc and infected cells. Cellular and viral lipids were extracted from isolated HCVcc and from uninfected and infected Huh-7 cells. Cholesterol content was determined using the cholesterol oxidase method as previously described (14). Total phospholipid content was determined using the method of Rouser et al. (42).

Cholesterol depletion and replacement. To remove cholesterol from the HCV envelope, stock samples of HCVcc were treated with *methyl*-β-cyclodextrin (B-CD) in DMEM (Sigma) supplemented with 10% fetal bovine serum (Sigma) and nonessential amino acids (Invitrogen, Carlsbad, CA) for 1 h at 37°C, followed by centrifugation at 100,000 × *g* for 3 h to form a pellet, which was resuspended in 0.5 ml of the medium. In order to replenish cholesterol, the medium of HCVcc treated with 5 mg/ml B-CD was replaced with DMEM containing various concentrations of exogenous cholesterol (Sigma) and incubated for 1 h, followed by centrifugation to form a pellet. In order to perform HCVcc infection assays, Huh-7 cells were infected with HCVcc, with or without the treatment described above, for 1 h at 37°C and then washed as described above. Viral core protein levels in the cells and in the supernatant were quantified 72 h later using an HCV core enzyme-linked immunosorbent assay (Ortho-Clinical Diagnostics, Tokyo, Japan).

SMase treatment. HCVcc was treated with SMase at various concentrations in DMEM for 1 h at 37°C and was then centrifuged at 100,000 × *g* for 3 h to form a pellet, which was resuspended in 0.5 ml of medium for the infection assays.

HCVcc binding and internalization assays. To monitor binding, cells grown in a 6-well plate were preincubated for 1 h at 4°C, after which B-CD- or SMase-treated HCVcc was bound to the cells for 1 h at 4°C. As a measure of virus internalization, following the virus binding procedure, the cells were warmed to 37°C and maintained for 2 h, after which they were treated with 0.25% trypsin for 10 min at 37°C. Huh7-25, a CD81-negative Huh-7 subclone (3), was used to ensure removal of surface-bound virus by trypsin treatment. For both the binding and internalization assays, the resulting cells, as described above, were washed with ice-cold phosphate-buffered saline, followed by lysis with TRIzol reagent (Invitrogen). Cell-associated virus was quantified by measuring the amount of HCV RNA in the cell lysate by the real-time reverse transcription-PCR method (2, 34). Cells were treated with heparinase as previously described (33).

HCV replication assay in HCVcc-infected or replicon cells. HCV subgenomic replicon cells or cells infected with HCVcc were treated with various concentrations of inhibitors for 72 h. Total RNA was isolated from replicon cells using TRIzol reagent (Invitrogen), followed by quantification of HCV RNA by real-time reverse transcription-PCR as previously described (2, 34). Levels of core protein in the culture supernatants of HCVcc-infected cells were tested as described above.

Detection of cholesterol content of HCVcc. For [^{3}H]cholesterol labeling of viruses, HCVcc-infected or uninfected cells were incubated with 50 mCi of [1α,2α-^{3}H]cholesterol in DMEM for 24 h. Culture supernatants of the cells were incubated in the presence or absence of B-CD at 5 mg/ml for 1 h at 37°C, followed by ultracentrifugation on a 60% sucrose cushion. The virus-containing fractions and corresponding fractions from an uninfected culture were lysed in the buffer containing 1% Triton X-100 (TX-100), and radioactivity was quantified by scintillation counting. Radioactivities (in counts per minute) of HCVcc samples were determined by subtracting the radioactivity of uninfected cells from that of HCVcc-infected cells.

Metabolic labeling analysis of sphingolipid content. After 2 h of incubation with [^{14}C]serine (0.5 mCi/ml) in Opti-MEM (Invitrogen), the cells were lysed with 0.1% sodium dodecyl sulfate, and total lipid was extracted with chloroform-methanol (1:2, vol/vol). The extracts were spotted onto silica gel 60 plates (Merck, Darmstadt, Germany) and chromatographed with methyl acetate–1-propanol–chloroform–methanol–0.25% KCl (25:25:25:10:9, vol/vol). Radioactive spots were quantitatively detected by BAS 2000 (Fuji Film, Japan).

Membrane flotation assay. The membrane flotation assay was performed as previously described (46).

TABLE 1. Cholesterol and phospholipid contents of HCVcc and cells

Cell type or virus	Content (nmol/mg of protein)[a]		Chol/PL ratio
	Chol	PL	
Cells			
Uninfected	105.9 ± 10.4	253.2 ± 10.6	0.42
JFH-1 infected	116.5 ± 10.0	292.0 ± 18.4	0.40
Virus			
JFH-1	43.6 ± 2.4	33.8 ± 1.8	1.29
J6/JFH-1[b]	28.7 ± 4.8	22.7 ± 2.9	1.26

[a] Data are averages of three independent measurements ± standard deviations. Chol, cholesterol; PL, phospholipids.

[b] J6/JFH1 virus was produced from the pJ6/N2X-JFH1 construct and has structural proteins from the J6CF strain.

RESULTS

Critical role of virion-associated cholesterol. A role of virion-associated cholesterol in infectivity has been demonstrated for several enveloped viruses (4). However, little is known about the role of lipids associated with the virions of flaviviruses, including HCV, and their contribution to the viral life cycle. To determine the lipid composition of mature HCV virions, we extracted total lipid from HCVcc (JFH-1 and chimeric J6/JFH-1) prepared from the culture supernatants of cells infected with HCV, as well as the total cellular membrane fractions of uninfected and infected Huh-7 cells. The cholesterol and phospholipid contents were quantified, because these are the two major lipid constituents of biological membranes. The cholesterol-to-phospholipid molar ratio, which is known as a parameter of membrane viscosity (47), was significantly higher in virus samples (1.29 and 1.26 for JFH-1 and J6/JFH-1, respectively) than in cell membrane samples (0.40 and 0.42 for JFH-1-infected and uninfected cells, respectively) (Table 1). The ratios in viral samples were similar to or greater than those in mammalian plasma membranes, where most cellular cholesterol is found. Minimal contamination of the viral samples with extracellular microvesicles likely occurred, since only a small amount of lipid was detected in a sample prepared from the culture medium of uninfected cells (data not shown). Thus, it is likely that HCV virions are enriched with cholesterol during assembly and maturation.

To investigate a potential role for the particular lipid composition of HCV particles, HCVcc was treated with

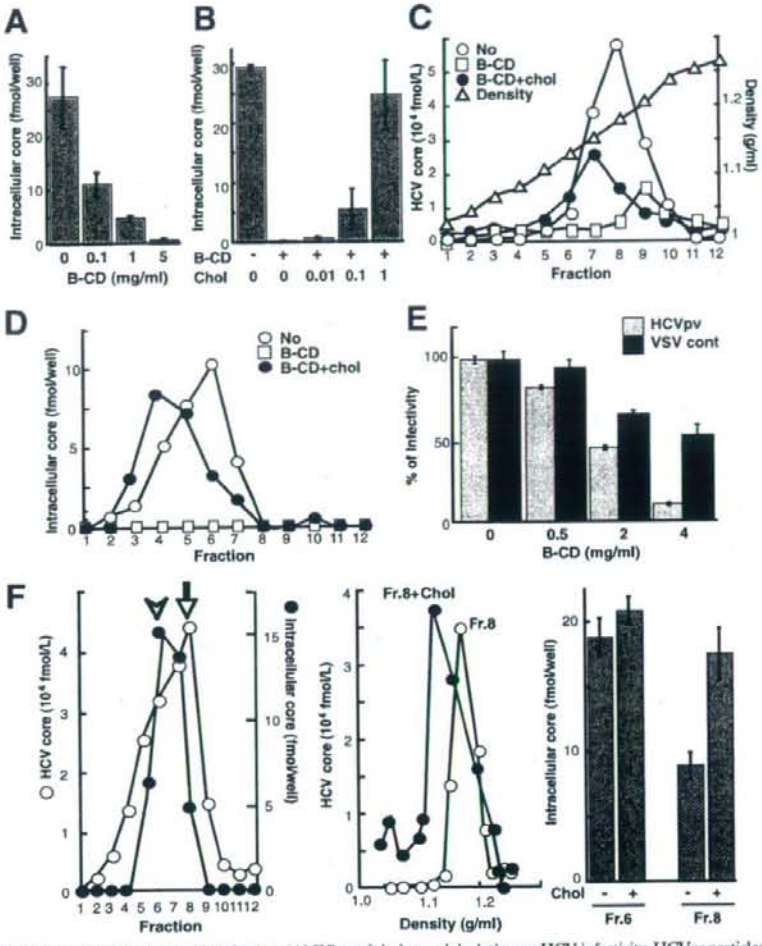

FIG. 1. Role of HCV-associated cholesterol in infection. (A) Effect of cholesterol depletion on HCV infectivity. HCVcc particles (~2 fmol of the core protein) were treated with B-CD at 0.1, 1, and 5 mg/ml for 1 h at 37°C. After removal of B-CD, Huh-7 cells were infected with the treated virus particles, after which the core protein content of infected cells at 72 h p.i. was determined as an indicator of infectivity, as previously established (24). (B) Effect of cholesterol replenishment on infectivity. After treatment with 5 mg/ml B-CD, virus was treated either with medium alone or with medium containing exogenous cholesterol for 1 h at 37°C. (C) Effect of cholesterol depletion and replenishment on density gradient profiles of the viral particles. The HCVcc treated with 5 mg/ml B-CD was replenished with exogenous cholesterol (1 mM) and then separated by 10-to-60% sucrose gradient ultracentrifugation. The core protein in each fraction was measured. The density of each fraction was determined by refractive index measurement. (D) Effects of cholesterol depletion and replenishment on viral infectivity. Each fraction (see panel C) was infected, and then the core proteins in the cells were measured at 72 h p.i. (E) Effect of cholesterol depletion on the infectivity of HCVpv (genotype 1a) (shaded bars) or the control, VSVdelG-GFP/G (solid bars). The viruses were preincubated with B-CD for 1 h at 37°C before infection. (F) (Left) The culture medium from HCVcc-producing cells was fractionated as described above. For each fraction, the amounts of core and intracellular core (infectivity) are plotted. Peaks of the core (arrow) and infectivity (arrowhead) are indicated. (Center) An aliquot of fraction 8 (peak of the core) was treated with 1 mM cholesterol for 1 h at 37°C. The resultant aliquot and an untreated aliquot of the fraction were subjected to sucrose gradient ultracentrifugation. The core in each fraction was plotted. (Right) The infectivities of fractions (Fr.) 6 and 8 (see the left panel) with or without cholesterol treatment were determined as shown above. Data are means from four independent experiments. Error bars, standard deviations.

increasing concentrations (0.1 to 5 mg/ml) of B-CD, which is known to extract cholesterol from membranes (40). The viral samples were then used to inoculate Huh-7 cells after removal of B-CD by ultracentrifugation. Infectivity was evaluated by quantifying the viral core protein in cells at 72 h postinfection (p.i.). Using an immunoassay that provides results indicative of HCV infectivity (25), we also confirmed a good correlation between the core level and

TABLE 2. Depletion of virion-associated cholesterol by B-CD

Treatment	Radioactivity (cpm) of HCVcc[a]		Avg (%[b])
	Expt 1	Expt 2	
None	5,327	5,573	5,450 (100)
B-CD (5 mg/ml)	3,643	1,646	2,644 (48.5)

[a] Determined by subtracting the radioactivity of uninfected cells from that of HCVcc-infected cells in two experiments.
[b] Percentage of the radioactivity of the untreated sample.

infectious titers (data not shown). As shown in Fig. 1A, core protein levels following B-CD treatment at 0.1, 1, or 5 mg/ml were reduced by 60, 83, or 98%, respectively, from the levels with the untreated virus. The cholesterol level of HCVcc treated with 5 mg/ml B-CD was found to be ~50% of that of untreated virions (Table 2).

To demonstrate that the reduced infection efficiency of B-CD-treated virus was caused by the reduced cholesterol content of the viral envelope, we attempted to reverse the inhibitory effect by adding exogenous cholesterol. Following treatment of HCVcc with 5 mg/ml B-CD, the drug was washed out, and increasing concentrations of cholesterol were added in an attempt to reconstitute the normal virion cholesterol content. The addition of 1 mM cholesterol completely reversed the virus infectivity (Fig. 1B). After cholesterol was replenished, the viral RNA was restored to a level similar to that in the untreated control.

To investigate the effect of cholesterol on the density of infectious HCV virions, B-CD-pretreated or untreated viral samples, as well as cholesterol-replenished treated viral samples, were subjected to sucrose density gradient centrifugation (Fig. 1C). The density of HCVcc core protein at its peak concentration in untreated virus samples was ~1.17 g/ml. When virion-associated cholesterol was removed by B-CD, the density of HCVcc core protein at its peak concentration was shifted to 1.20 g/ml. Addition of exogenous cholesterol to this cholesterol-depleted sample restored a lower-density fraction (1.15 g/ml). Figure 1D illustrates the infectivity of each gradient fraction. Untreated virus had maximum infectivity at ~1.13 g/ml (fraction 6), while, as expected, fractions from B-CD-treated viral samples exhibited minimal to no infectivity. Replenishment of depleted virus with cholesterol returned infectivity to untreated-control levels, and cholesterol-replenished virus had a buoyant density of ~1.07 g/ml (fraction 4), suggesting that HCV-associated cholesterol is crucial for viral infectivity and that the effect of a cholesterol-depleting drug is reversible. We further observed that B-CD treatment of a pseudotyped VSV containing the E1 and E2 proteins of the HCV genotype 1a isolate H77c (HCVpv) resulted in a progressive loss of infectivity, while B-CD had significantly less impact on the infectivity of the control virus VSVdelG-GFP/G (Fig. 1E).

The results described above raise the possibility that the infectivity of HCV virions with relatively low levels of incorporated cholesterol might be enhanced by supplementation with exogenous cholesterol. Density gradient fractions of culture supernatants collected from HCV-infected cells were analyzed with regard to the presence of core protein and infectivity (Fig. 1F, left). As indicated above, maximum infectivity was obtained with fraction 6 (1.13 g/ml). In contrast, a major fraction of core protein banded at a higher density (1.17 g/ml) in fraction 8. We hypothesized that fraction 8 contains lipids at lower levels than those in fraction 6. However, quantification of lipids, including cholesterol, in the fractions obtained failed, presumably due to a low sensitivity of detection. Thus, to extend our findings on the involvement of cholesterol, we added exogenous cholesterol to fraction 8, followed by ultrafiltration to remove unincorporated cholesterol. A subsequent density gradient profile demonstrated a shift in the core protein peak to 1.13 g/ml (Fig. 1F, center). A concomitant increase in the infectivity of the fraction, approaching that of untreated fraction 6, was observed (Fig. 1F, right). In contrast, supplementation of fraction 6 with exogenous cholesterol did not alter its infectivity (Fig. 1F, right) or change its density gradient (data not shown). These results suggest that exogenous cholesterol supplementation can reverse deficits in the infectivity of HCV virions due to low cholesterol content.

Sphingolipid dependence of HCV infectivity. In addition to cholesterol, sphingolipid is a major component of eukaryotic lipid membranes. We therefore investigated the functional significance of sphingomyelin (SM), the most abundant sphingolipid, with regard to HCV infectivity. HCVcc was treated for 1 h with increasing concentrations (0.1 to 10 U/ml) of bacterial SMase, which is known to hydrolyze membrane-bound SM to ceramide. Following ultracentrifugation to remove the SMase, Huh-7 cells were inoculated with the HCVcc. The amount of HCV core protein within the cells was quantified at 72 h p.i. Figure 2A shows 50 and 90% reductions in HCV infectivity after incubation of the virion with 0.1 and 1 U/ml SMase, respectively. We further observed that SMase treatment of HCVpv resulted in a progressive loss of infectivity, while SMase had no effect on the infectivity of the control virus (Fig. 2B). This demonstrates that sphingolipid, like cholesterol, plays an essential role in HCV infectivity.

Requirement for virion-associated cholesterol and sphingolipid during HCV cell entry. These findings support the idea that virion-associated cholesterol and sphingolipid may influence viral entry into host cells by altering the interaction between viral particles and a host cell factor(s). Viral entry is a multistep process including binding of the virion to the cell surface and internalization into the cytoplasm by endocytosis. To examine whether virion-associated cholesterol and SM might play a role in cell binding or postbinding events during viral entry, we used a binding assay in which Huh-7 cells preincubated for 1 h at 4°C were infected with B-CD- or SMase-treated HCVcc. Total RNA was extracted after a 1-h addition of the virions at 4°C, followed by quantification of HCV RNA. As shown in Fig. 3A, treatment of the virions with either B-CD or SMase had little influence on their ability to bind to cells.

It has been shown that CD81 plays an important role in HCV internalization but is not correlated with viral attachment (7, 33). An anti-CD81 antibody was used as a negative control for reduced viral attachment. It is likely that heparan sulfate proteoglycan on the target cell surface is needed for the initial attachment of HCV (33). Thus, heparinase I was used as a positive control for reduced HCV attachment to the cells. To examine the roles of cholesterol and sphingolipid on the HCVcc membrane in viral internalization, a virus-cell mixture

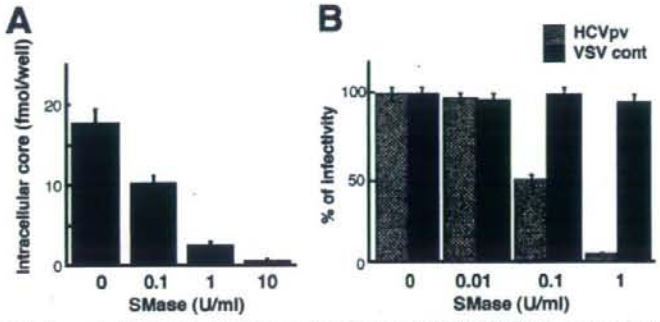

FIG. 2. Effect of SM hydrolysis on viral infectivity. (A) Effect on the infectivity of HCVcc. HCVcc was treated with 0.1, 1, or 10 U/ml SMase for 1 h at 37°C, after which SMase was removed by ultracentifugation. Huh-7 cells were infected with the treated virus, and the core protein content of infected cells was determined at 72 h p.i. (B) Effect on the infectivity of HCVpv (genotype 1a) (shaded bars) or the control, VSVdelG-GFP/G (VSV cont) (solid bars). The viruses were preincubated with SMase for 1 h at 37°C before infection. Data are means from four independent experiments. Error bars, standard deviations.

prepared at 4°C as described above was incubated for 2 h at 37°C, followed by trypsinization to remove virions that were surface bound but not internalized (Fig. 3B). We verified that 94% of surface-bound-viruses were removed by trypsinization using CD81-negative Huh-7 subclones. A marked reduction in viral RNA levels within cells was detected after pretreatment of the virus with either B-CD or SMase. These results strongly suggest that virion-associated cholesterol and sphingolipid function as key determinants of internalization but not of cell attachment.

Association of HCV structural proteins with lipid rafts. Cholesterol and sphingolipid are major components of lipid rafts, which can be isolated as detergent-resistant membranes (DRMs) by treatment with cold TX-100, followed by equilibrium flotation centrifugation. Matto et al. (30) reported that HCV core protein is associated with DRMs in cells carrying the full-length HCV replicon. To investigate whether HCV structural proteins are associated with DRMs in HCVcc-producing cells, lysates from cells infected with HCVcc were subjected to membrane flotation analysis. In the absence of detergent treatment, the majority of the core (Fig. 4A) and E1 (Fig. 4B) proteins were detected in the membrane fractions. After treatment with cold TX-100, significant amounts of both viral proteins were recovered from the DRM fraction. However, after treatment with TX-100 at 37°C, the majority of the E1 and core proteins had shifted to the detergent-soluble fractions. We also found that HCV genotype 1b E1 and E2 can be associated with the lipid raft in 293T cells transfected with an E1 or E2 expression plasmid (Fig. 4C) and that the cytoplasmic tails of envelope

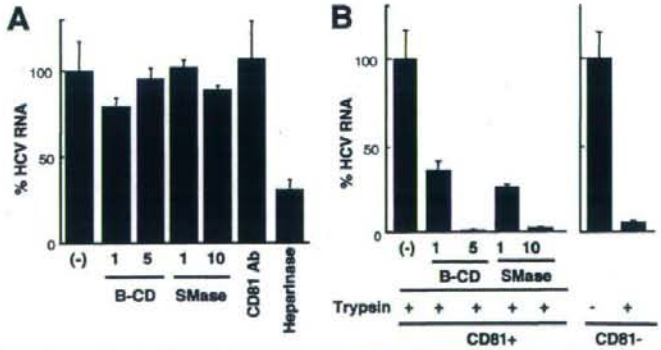

FIG. 3. Effects of B-CD or SMase on virus attachment and internalization. (A) Virus attachment to Huh-7 cells was determined at 4°C after treatment of HCVcc with B-CD (1 or 5 mg/ml) or SMase (1 or 10 U/ml). An antibody (Ab) against CD81 was used, in order to ensure that the antibody did not inhibit HCVcc binding (7, 33). Heparinase was used to reduce HCV attachment to the cell. Viral RNA copies were normalized to total cellular RNA, and the normalized RNA copies in the mock-treated sample (−) were arbitrarily set at 100%. (B) Virus internalization was measured in Huh7-25, a CD81-negative subclone ($CD81^-$) (3), and Huh7-25-CD81, which stably expresses CD81 ($CD81^+$), after treatment of the virions with B-CD or SMase. After internalization for 2 h at 37°C, cells were exposed to trypsin (trypsin +) or phosphate-buffered saline (trypsin −). Huh7-25 was used to ensure that surface-bound virus would be removed by trypsin treatment. The amounts of HCV RNA in Huh7-25 and Huh7-25-CD81 cells infected with untreated HCVcc were assigned the arbitrary value of 100%, respectively. Results are representative of four independent experiments.